ISSN 1674-1056
http://cpb.iphy.ac.cn
http://iopscience.iop.org/cpb
中国物理 B
Chinese Physics
中国物理 Chinese Physics B

Thickness-dependent excitonic properties of atomically thin 2H-$MoTe_2$

Jin-Huan Li(李金焕)[1], Dan Bing(邴单)[1], Zhang-Ting Wu(吴章婷)[3], Guo-Qing Wu(吴国庆)[1], Jing Bai(白静)[1], Ru-Xia Du(杜如霞)[1], Zheng-Qing Qi(祁正青)[2]

Citation: Chin. Phys. B . 2020, 29(1): 017802 . **doi:** 10.1088/1674-1056/ab5a3a
Journal homepage: http://cpb.iphy.ac.cn; http://iopscience.iop.org/cpb

What follows is a list of articles you may be interested in

Photoluminescence properties of blue and green multiple InGaN/GaN quantum wells

Chang-Fu Li(李长富), Kai-Ju Shi(时凯居), Ming-Sheng Xu(徐明升), Xian-Gang Xu(徐现刚), Zi-Wu Ji(冀子武)
Chin. Phys. B . 2019, 28(10): 107803 . **doi:** 10.1088/1674-1056/ab4046

Increase of photoluminescence blinking frequency of 3C-SiC nanocrystals with excitation power

Zhixing Gan(甘志星), Weiping Zhou(周卫平), Ming Meng(孟明)
Chin. Phys. B . 2018, 27(12): 127804 . **doi:** 10.1088/1674-1056/27/12/127804

Photodynamics of Ga_{Zn}-V_{Zn} complex defect in Ga-doped ZnO

Ai-Hua Tang(汤爱华), Zeng-Xia Mei(梅增霞), Yao-Nan Hou(侯尧楠), Xiao-Long Du(杜小龙)
Chin. Phys. B . 2018, 27(11): 117802 . **doi:** 10.1088/1674-1056/27/11/117802

Recent progress on photoluminescence from plasmonic nanostructures: Phenomenon, mechanism, and application

Tingting Yin(尹婷婷), Liyong Jiang(蒋立勇), Zexiang Shen(申泽骧)
Chin. Phys. B . 2018, 27(9): 097803 . **doi:** 10.1088/1674-1056/27/9/097803

Transition intensity calculation of Yb: YAG

Hong-Bo Zhang(张洪波), Qing-Li Zhang(张庆礼), Xing Wang(王星), Gui-Hua Sun(孙贵花), Xiao-Fei Wang(王小飞), De-Ming Zhang(张德明), Dun-Lu Sun(孙敦陆)
Chin. Phys. B . 2018, 27(6): 067801 . **doi:** 10.1088/1674-1056/27/6/067801

Thickness-dependent excitonic properties of atomically thin 2H-$MoTe_2$*

Jin-Huan Li(李金焕)[1], Dan Bing(邴单)[1], Zhang-Ting Wu(吴章婷)[3], Guo-Qing Wu(吴国庆)[1], Jing Bai(白静)[1], Ru-Xia Du(杜如霞)[1], and Zheng-Qing Qi(祁正青)[2,†]

[1] *Department of Basic Teaching, Nanjing Tech University Pujiang Institute, Nanjing* 211134, *China*

[2] *School of Network and Communication Engineering, Jinling Institute of Technology, Nanjing* 211169, *China*

[3] *Lab for Nanoelectronics and NanoDevices, Department of Electronics Science and Technology, Hangzhou Dianzi University, Hangzhou* 310018, *China*

(Received 20 October 2019; revised manuscript received 19 November 2019; accepted manuscript online 22 November 2019)

Two-dimensional (2D) 2H-$MoTe_2$ is a promising semiconductor because of its small bandgap, strong absorption, and low thermal conductivity. In this paper, we systematically study the optical and excitonic properties of atomically thin 2H-$MoTe_2$ (1–5 layers). Due to the fact that the optical contrast and Raman spectra of 2H-$MoTe_2$ with different thicknesses exhibit distinctly different behaviors, we establish a quantitative method by using optical images and Raman spectra to directly identify the layers of 2H-$MoTe_2$ thin films. Besides, excitonic states and binding energy in monolayer/bilayer 2H-$MoTe_2$ are measured by temperature-dependent photoluminescence (PL) spectroscopy. At temperature $T = 3.3$ K, we can observe an exciton emission at ~ 1.19 eV and trion emission at ~ 1.16 eV for monolayer 2H-$MoTe_2$. While at room temperature, the exciton emission and trion emission both disappear for their small binding energy. We determine the exciton binding energy to be 185 meV (179 meV), trion binding energy to be 20 meV (18 meV) for the monolayer (bilayer) 2H-$MoTe_2$. The thoroughly studies of the excitonic states in atomically thin 2H-$MoTe_2$ will provide guidance for future practical applications.

Keywords: 2H-$MoTe_2$, photoluminescence, Raman, exciton and trion

PACS: 78.67.–n, 78.55.–m, 74.25.nd **DOI:** 10.1088/1674-1056/ab5a3a

1. Introduction

Atomically thin transition metal dichalcogenides (TMDs) have recently attracted great attention for their special electronic and optical properties.[1–3] The atoms of TMDs are held together by strong covalent in-plane bonds but are oriented in the out-of-plane direction by weak van der Waals forces. Thus, few layered two-dimensional (2D) materials can be easily exfoliated from bulk crystal materials.[4,5] When these materials are thinned down to a single layer, the indirect band gap will transform into direct band gap,[6–8] this transformation not only enhances the quantum yield of photoluminescence (PL),[9] but also is a necessary condition for the observation of Valley Hall effect.[10–12] In some TMDs, the indirect–direct bandgap transition between bulk and single layer provides a variety of optoelectronic applications ranging from photodetectors to light emitters.[13] The thickness of 2D materials strongly affects their optical, electronic, and other properties. In order to investigate the properties of 2D materials, it is necessary to identify the thickness quickly.

2H-$MoTe_2$ is a new material, its layer-dependent bandgap ranges from 0.8 eV (bulk) to 1.1 eV (monolayer) as the thickness decreases and it exhibits direct-to-indirect bandgap transition.[14] The bandgap feature of 2H-$MoTe_2$ flake suggests that it is favorable for visible and SWIR photodetection.[15–17] Other distinctive properties have also been addressed in 2H-$MoTe_2$. Its mobility at room temperature (RT), for example, can theoretically reach up to 200 $cm^2 \cdot V^{-1} \cdot s^{-1}$.[18] The gate voltage of several volts can drive phase transition from semiconductor to semimetal in monolayer 2H-$MoTe_2$ by choosing appropriate dielectrics. With its unique properties, 2H-$MoTe_2$ has a promising application in the fields of optoelectronics, energy storage, memristor, chemical and biological sensing, *etc.*[19–21] In recent years, the optical properties of 2H-$MoTe_2$ have been studied.[22] For example, the optical contrast,[23,24] PL and Raman spectra[25,26] have been observed. However, a systematically study in using these thickness-dependent properties to identify the layer number of 2H-$MoTe_2$ is lacking. Moreover, owing to the spatial confinement and reduced dielectric screening, noticeable exciton effects are widely expected in monolayer crystals of TMDs.[27] Numerous experimental and theoretical investigations of neutral excitons and charged excitons (trions) have been conducted in 2D TMD semiconductors.[28,29] Most of these investigations focused on atomically thin MX_2 (X = Se, S; M = W, Mo) 2D semiconductors. However, researches of the exciton binding energy in atomically thin 2H-$MoTe_2$, which are of great significance for developing the novel 2H-$MoTe_2$ based excitonic devices, are still lacking.

In this work, we systematically analyze the optical prop-

*Project supported by the Natural Science Research Projects in Colleges and Universities of Jiangsu Province, China (Grant No. 18KJD140003).

†Corresponding author. E-mail: qi.zq@163.com

© 2020 Chinese Physical Society and IOP Publishing Ltd

erties of mechanically exfoliated atomically thin 2H-$MoTe_2$ by using atomic force microscope (AFM), optical contrast, and Raman spectroscopy. We identify the thickness of 1L–5L 2H-$MoTe_2$ flake. Temperature-dependent PL measurement is used to determine the optical band gap and to probe excitonic states in few-layer 2H-$MoTe_2$. From the PL spectra, we find that 2H-$MoTe_2$ possesses a direct optical band gap of 1.19 eV. Therefore, 2H-$MoTe_2$ is a new direct band gap 2D material, and its band gap is significantly lower than those of other TMDs available heretofore. More importantly, we obtain the exciton (trion) binding energy in monolayer/bilayer 2H-$MoTe_2$.

2. Sample preparation

We used mechanical exfoliation to obtain atomically thin 2H-$MoTe_2$ from bulk crystals (SPI Supplies) and transferred it into an Si wafer capped with a 300-nm-thick SiO_2 layer. The exfoliation process was carried out in ambient air at room temperature. After exfoliation, tape residue was removed by being soaked in acetone, then rinsed with isopropanol and blow-dried with N_2. The AFM was utilized to identify the thickness of 2H-$MoTe_2$ as shown in Fig. 1. Figures 1(a) and 1(b) show the optical images of 2H-$MoTe_2$ sample and the AFM curves traced with the red dashed line. The AFM curve shows that the step height from substrate to monolayer is about 1 nm, while the step height between the adjacent layers is about 0.7 nm each layer, consistent with previous measurements.[30] The larger step height difference above is possibly caused by the reflection changes between the substrate and the sample and also the presence of several adsorbates on the substrate.[31,32]

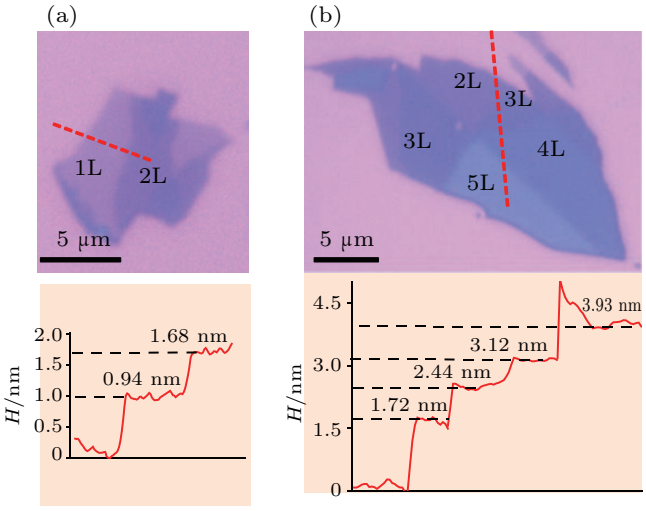


Fig. 1. (a) and (b) Optical microscope image and AFM curve (along the red dashed lines) of 2H-$MoTe_2$ flakes.

3. Results and discussion

To further optically illustrate the layer number, the R, G, and B channel images of the optical image (Fig. 2(a)) are obtained by Matlab software,[31] and shown in Figs. 2(b)–2(d). It can be seen that the optical contrast of 2H-$MoTe_2$ sample varies with thickness obviously in the R channel (Fig. 2(b)) and G channel (Fig. 2(c)). However, in the B channel (Fig. 2(d)), the optical contrast is hard to distinguish between 2H-$MoTe_2$ sample and substrate. To quantify the optical contrast as shown in Fig. 2(e), the variation of the contrast value with layer thickness is measured with an optical microscope. The contrast value C is calculated from the equation $C = (C_{sub} - C_{sam})/C_{sub.}$ Here, C_{sub} is the contrast value taken from the substrate, and C_{sam} is the contrast value taken from the 2H-$MoTe_2$ sample.[33] The contrast values of R channel are 0.22 (1L), 0.34 (2L), 0.42 (3L), 0.45 (4L), and 0.39 (5L), respectively. For 1–3 layers of 2H-$MoTe_2$, the contrast value of R channel increases linearly. The contrast of G channel decreases linearly with 3–5 layers. For 2H-$MoTe_2$ samples with different layers, the change of contrast value of B channel is not obvious, so the number of layers of 2H-$MoTe_2$ can be identified by the contrast between R channel and G channel.

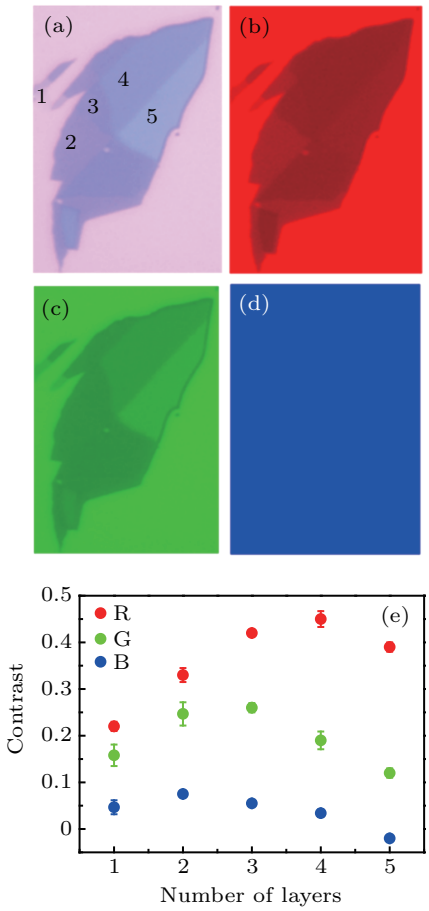


Fig. 2. (a) Optical image of 2H-$MoTe_2$ sample obtained with mechanical exfoliation; (b)–(d) R, G, and B channel images of 2H-$MoTe_2$ sample; (e) optical contrast values of 2H-$MoTe_2$ samples with different thicknesses.

Raman spectroscopy as a noninvasive method can also be used to measure the thickness of 2D material.[34] Figure 3(a) shows three typical Raman modes of 2H-$MoTe_2$: the out-of-plane A_{1g} mode (~ 170 cm^{-1}), the in-plane E^1_{2g} mode (~ 233 cm^{-1}), and the B^1_{2g} phonon mode (~ 290 cm^{-1}).[24] The position of the A_{1g} peak and the E^1_{2g} peak upshift with

thickness decreasing (Fig. 3(b)), the change in the peak position is due to the effect of boundary surface and interlayer interaction with thickness decreasing. Furthermore, a strong peak at $\sim 290\ \mathrm{cm}^{-1}$ emerges in the atomically thin 2H-$MoTe_2$. This peak is not observed in the bulk nor monolayer 2H-$MoTe_2$ crystal, but the intensity is very strong in bilayer and decreases with thickness increasing. In Fig. 3(c), it seems that the A_{1g} mode of 3L–5L 2H-$MoTe_2$ exhibits multiple peaks, which is well known as Davydov splitting in bulk and bilayer TMDs.[35,36] The generation of Dovydov splitting can be attributed to the interaction between layers. In addition, with the increase of layers' number, the A_{1g} peak is blue-shifted. According to Fig. 3(d), the intensity ratios of B^1_{2g}/E^1_{2g} for 2–5 layers are 0.37, 0.22, 0.19, and 0.15, respectively, their changes with layer are obvious. Therefore, the layers of 2H-$MoTe_2$ can also be determined by the intensity ratio of B^1_{2g}/E^1_{2g}. The dependence of the peak position of E^1_{2g} mode on thickness is also studied as shown in the inset, it is found that the E^1_{2g} mode is shifted up by $1.5\ \mathrm{cm}^{-1}$, with thickness decreasing from five layers to a single layer.

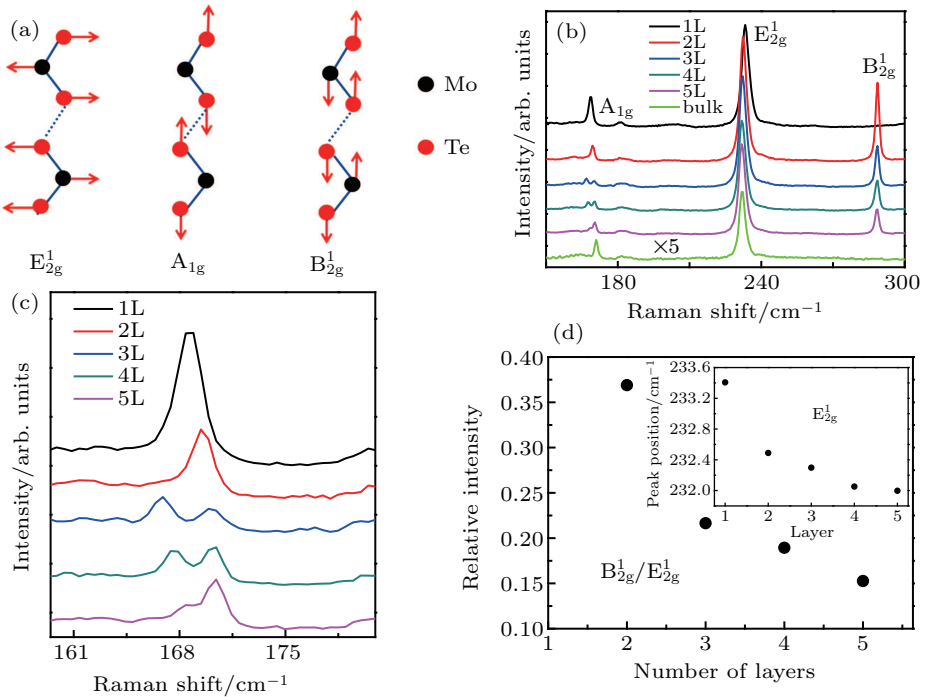


Fig. 3. (a) Three Raman-active vibration modes of layered 2H-$MoTe_2$, E^1_{2g}, A_{1g}, and B^1_{2g} respectively, (b) Raman spectra of 1L–5L and bulk 2H-$MoTe_2$, (c) A_{1g} modes in 1L–5L 2H-$MoTe_2$, (d) intensity ratio of B^1_{2g}/E^1_{2g} *versus* number of layers, with inset showing the peak position of the E^1_{2g} mode as a function of thickness.

Figures 4(a) and 4(b) display the photoluminescence (PL) spectra of monolayer and bilayer 2H-$MoTe_2$ varying with temperature, respectively. The power and wavelength of incident laser are, respecectively, 100 μW and 532 nm for Raman and PL measurement. At 3.3 K, the 1L 2H-$MoTe_2$ exhibits two PL peaks at about 1.16 eV and 1.19 eV, which have been studied and assigned to the emission from trion and exciton, respectively.[37] At room temperature, we observed no PL of 2H-$MoTe_2$, which is mainly because of its small binding energy, vulnerable to external environment (such as tem perature). With the increase of temperature, electrons or holes change from exciton radiation recombination to non-radiation recombination due to thermal disturbance, the intensities of neutral and charged exciton peaks appear at low temperature gradually decrease with temperature increasing, and almost disappear at 150 K. When the temperature exceeds 60 K, it mainly comes from neutral exciton luminescence, for the binding energy of neutral exciton is larger than that of charged exciton.[29] From the difference in energy between the exciton peak and trion peak, we can calculate the trion binding energy (Figs. 4(c) and 4(d)). The binding energy values of the monolayer and bilayer charged exciton of 2H-$MoTe_2$ are 21 meV and 19 meV, respectively. The binding energy of charged exciton in other ultra-thin 2D semiconductors have also been reported, such as 30 meV for monolayer $MoSe_2$, 18 meV for monolayer MoS_2, and 30 meV for bilayer WSe_2.[37–39] In addition, with the increase of temperature, all peaks of 2H-$MoTe_2$ in monolayer and bilayer are red-shifted, mainly because the band gap decreases with the increase of temperature. The relationship between band gap and temperature is as follows:[40] $E_g(T) = E_g(0) - S\langle\hbar\omega\rangle\left[\coth\left(\langle\hbar\omega\rangle/2k_BT\right)\right]$. Here $E(0)$ is the bandgap at $T = 0$ K, S is the dimensionless constant, $\langle\hbar\omega\rangle$ represents the average acoustic phonon energy involved in the electron-phonon interaction, and k_B is the Boltzmann constant. As the temperature increases, $E_g(T)$ decreases gradually, so the PL peak exhibits the red shift. Exciton–phonon interaction has an important influence on the movement of exciton peak. When the exciton moves in the

lattice, it will interact with the phonon through the scattering. With the increase of temperature, the scattering increases. Therefore, the exciton energy changes due to the exciton–phonon interaction.

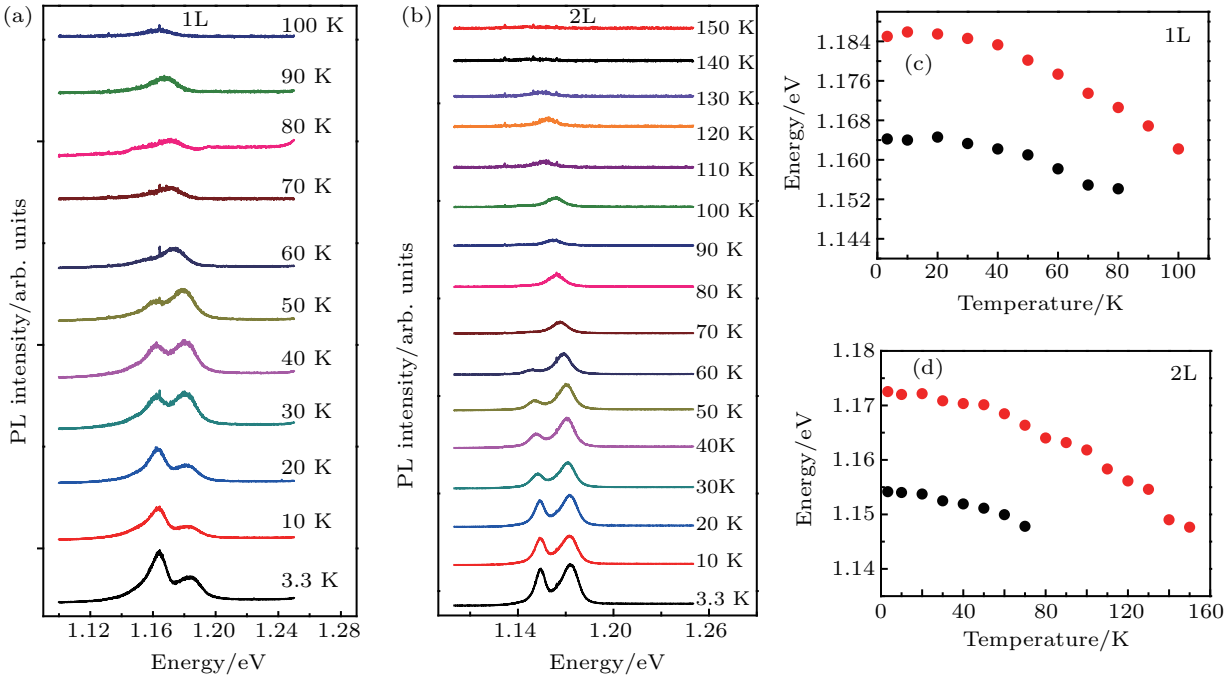


Fig. 4. PL spectra of (a) 1L and (b) 2L 2H-$MoTe_2$ *versus* temperature, exciton and trion peak positions of mono (c) and bilayer (d) 2H-$MoTe_2$ as a function of temperature.

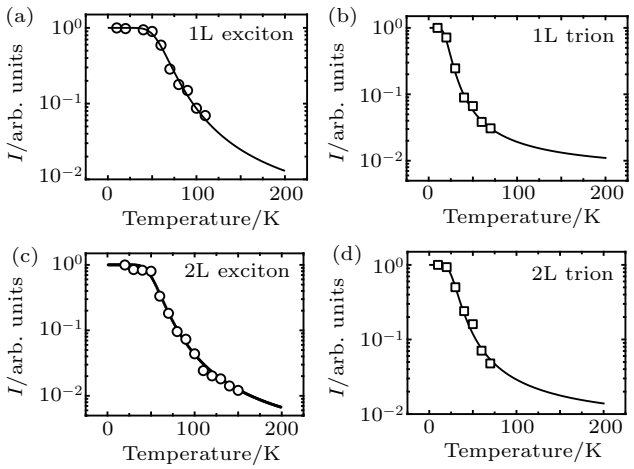


Fig. 5. Plots of exciton and trion intensities *versus* temperature, where solid lines are fits to data by using thermal dissociation model.

Figure 4 shows that the PL intensity of neutral and charged exciton decrease with temperature increasing. In the case of steady state, we can consider that the change of exciton intensity with temperature is mainly a reflection of the exciton population, and the excitons are in complete thermal equilibrium. The process of thermal dissociation can be used to describe the change of exciton population (N) with temperature T:[41] $N(T) = N_0/(1 + (\tau/\tau_0)\,\mathrm{e}^{-E_\mathrm{A}/k_\mathrm{B}T})$ where N_0 is the population of excitons at 0 K (*i.e.*, peak intensity), τ is the lifetime of excitons, τ_0 is the effective scattering time, and E_A is the activation energy. E describes the necessary energy for the thermal quenching of exciton luminescence. Fitting the data of PL peak intensity *versus* temperature (Figs. 4(a) and 4(b)) with this equation, we obtain $E = 185$ meV and 20 meV (179 meV and 18 meV) for the exciton and trion in monolayer (bilayer) (Fig. 5), respectively. This result is reasonable compared with that from similar TMDs like monolayer WSe_2 (210 meV).[42]

4. Conclusions

In this work, we study the optical properties of atomically thin 2H-$MoTe_2$ to identify the layers directly. This identification utilizes the layer-dependence of the optical contrast, and Raman spectra of 2H-$MoTe_2$ will provide a fast, nondestructive, easy-to-use, and accurate method to identify the number of 2H-$MoTe_2$ layers. By analyzing the temperature-dependent PL spectra, the excitonic states and exciton binding energy values of single-layer and double-layer) 2H-$MoTe_2$ are investigated. The exploration of the excitonic state in 2H-$MoTe_2$ is an important step towards materials optimization for the near-infrared photodetection.

References

[1] Guo X T, Wang W H, Nan H Y, Yu Y F, Jiang J, Zhao W W, Li J H, Zafar Z, Xiang N, Ni Z H, Hu W D, You Y M and Ni Z H 2016 *Optica* **3** 1066
[2] Du R X, Wang W H, Du J X, Guo X T, Liu E, Bing D and Bai J 2016 *Appl. Phys. Express* **9** 115101
[3] Zhang H, Cheng H M and Ye P D 2018 *Chem. Soc. Rev.* **47** 6009
[4] Lv R T, Robinson J, Schaak R, Sun D, Sun Y F, Mallouk T and Terrones M 2014 *Acc. Chem. Res.* **48** 56
[5] Splendiani A, Sun L, Zhang Y, Li T, Kim J, Chim C Y, Galli G and Wang F 2010 *Nano Lett.* **10** 1271
[6] Zhao W, Ghorannevis Z, Chu L, Toh M, Kloc C, Tan P H and Eda G 2012 *ACS Nano* **7** 791

[7] Tongay S, Zhou J, Ataca C, Lo K, Matthews T S, Li J, Grossman J C and Wu J 2012 *Nano Lett.* **12** 5576

[8] Zhang Y, Chang T R, Zhou B, Cui Y T, Yan H, Liu Z, Schmitt F, Lee J, Moore R, Chen Y, Lin H, Jeng H T, Mo S K, Hussain Z, Bansil A and Shen Z X 2014 *Nat. Nanotechnol.* **9** 111

[9] Lezama I G, Arora A, Ubaldini A, Barreteau C, Giannini E, Potemski M and Morpurgo A F 2015 I *Nano Lett.* **15** 2336

[10] Cao T, Wang G, Han W, Ye H, Zhu C, Shi J, Niu Q, Tan P, Wang E, Liu B and Feng J 2012 *Nat. Commun.* **3** 887

[11] Mak K F, He K, Shan J and Heinz T F 2012 *Nat. Nanotechnol.* **7** 494

[12] Zhang Y J, Oka T, Suzuki R, Ye J T and Iwasa Y 2014 *Science* **344** 725

[13] Eda G and Maier S A 2013 *ACS Nano* **7** 5660

[14] Yang J, Lü T, Myint Y W, Pei J, Macdonald D, Zheng J C and Lu Y 2015 *ACS Nano* **9** 6603

[15] Huang H, Wang J, Hu W, Liao L, Wang P, Wang X, Gong F, Chen Y, Wu G, Luo W, Shen H, Lin T, Sun J, Meng X, Chen X and Chu J 2016 *Nanotechnology* **27** 445201

[16] Octon T, Nagareddy V, Russo S, Craciun M and Wright C 2016 *Adv. Opt. Mater.* **4** 1750

[17] Yu W, Li S, Zhang Y, Ma W, Sun T, Yuan J, Fu K and Bao Q 2017 *Small* **13** 1700268

[18] Conan A, Bonnet A, Zoaeter M and Ramoul D 1984 *Phys. Status Solidi B* **124** 403

[19] Lin Y F, Xu Y, Wang S T, Li S L, Yamamoto M, Aparecido-Ferreira A, Li W, Sun W H, Nakaharai S and Jian W B 2014 *Adv. Mater.* **26** 3263

[20] Feng Z, Xie Y, Chen, J, Yu Y, Zheng S, Zhang R and Pang W 2017 *2D Materials* **4** 025018

[21] Sun L, Ding M, Li J, Yang L, Lou X, Xie Z, Chang H 2019 *Appl. Surf. Sci.* **496** 143687

[22] Li Y, Duerloo K A, Wauson K and Reed E J 2016 *Nat. Commun.* **7** 10671

[23] Ruppert C, Aslan O B and Heinz T F 2014 *Nano Lett.* **14** 6231

[24] Yamamoto M, Wang S T, Ni M, Lin Y F, Li S L, Aikawa S, Jian W B, Ueno K, Wakabayashi K and Tsukagoshi K 2014 *ACS Nano* **8** 3895

[25] Guo H H, Yang T, Yamamoto M, Zhou L, Ishikawa R, Ueno K, Tsukagoshi K, Zhang Z D, Dresselhaus M S and Saito R 2015 *Phys. Rev. B* **91** 205415

[26] Grzeszczyk M, Gołasa K, Zinkiewicz M, Nogajewski K, Molas M R, Potemski M, Wysmołek A and Babiński A 2016 *2D Material* **3** 025010

[27] Qiu D Y, da Jornada F H and Louie S G 2013 *Phys. Rev. Lett.* **111** 216805

[28] Berkelbach T, Hybertsen M and Reichman D 2013 *Phys. Rev. B* **88** 045318

[29] Zhu B, Chen X, Cui X 2015 *Sci. Rep.* **5** 9218

[30] Chang Y M, Lin C Y, Lin Y F, and Tsukagoshi K 2016 *Jpn. J Appl. Phys.* **55** 1102A1

[31] Nemes-Incze P, Osvath Z, Kamaras K and Biro L P 2008 *Carbon* **46** 1435

[32] Lee C, Yan H, Brus L E, Heinz T F, Hone J and Ryu S 2010 *ACS Nano* **4** 2695

[33] Wang Y Y, Gao R X, Ni Z H, He H, Guo S P, Yang H P, Cong C X and Yu T 2012 *Nanotechnology* **23** 495713

[34] Ni Z H, Wang Y Y, Yu T and Shen Z X 2008 *Nano Res.* **1** 273

[35] Song Q J, Tan Q H, Zhang X, Wu J B, Sheng B W, Wan Y, Wang X Q, Dai L and Tan P H 2016 *Phys. Rev. B* **93** 115409

[36] Kim S, Kim K, Lee J U and Cheong H 2017 *2D Materials* **4** 045002

[37] Ross J S, Wu S, Yu H, Ghimire N J, Jones A M, Aivazian G, Yan J, Mandrus D G, Xiao D, Yao W and Xu X 2013 *Nat. Commun.* **4** 1474

[38] Mak K F, He K, Lee C, Lee G H, Hone J, Heinz T F and Shan J 2013 *Nat. Mater.* **12** 207

[39] Jones A M, Yu H, Ross J S, Klement P, Ghimire N J, Yan J Q, Mandrus D G, Yao W and Xu X D 2014 *Nat. Phys.* **10** 130

[40] Huang J, Hoang T B and Mikkelsen M H 2016 *Sci. Rep.* **6** 22414

[41] Kulyuk L, Charron L and Fortin E 2003 *Phys. Rev. B* **68** 075314

[42] Zhang Y, Ugeda M M, Jin C H, Shi S F, Bradley A J, Martín-Recio A and Zhou B 2016 *Nano Lett.* **16** 2485